Nonlinear dynamic analyses of a cable-net glass façade under earthquake excitation

18TH WORLD CONFERENCE ON EARTHQUAKE ENGINEERING
WCEE2024
MILAN

MILAN, ITALY
30TH JUNE - 5TH JULY 2024
www.wcee2024.it

NONLINEAR DYNAMIC ANALYSES OF A CABLE-NET GLASS FAÇADE UNDER EARTHQUAKE EXCITATION

A. Reggio[1], G. Brancasi[1], G. Manara[2], F. Occhineri[2], M. Corrado[1]

[1] Department of Structural, Geotechnical and Building Engineering, Politecnico di Torino, Torino, Italy, anna.reggio@polito.it; giorgio.brancasi@studenti.polito.it; mauro.corrado@polito.it

[2] Permasteelisa S.p.A., Vittorio Veneto, Italy, g.manara@permasteelisagroup.com; f.occhineri@permasteelisagroup.com

Abstract: *Cable-net glass façades are the unique trait of an increasing number of modern iconic architectures (e.g., Market Hall, Rotterdam; Sony Centre, Berlin). This façade system, composed of glazing units supported by a net of orthogonal pre-tensioned steel cables, meets several architectural demands such as a minimal supporting system and a remarkable transparency of the building envelope, an efficient use of natural lighting, a peculiar aesthetic value. Issues may arise, however, due to the high flexibility of the cables and the deflections, possibly very large, of the façade under horizontal loadings (wind, earthquake). Therefore, a cable-net façade could be a major contributor to non-structural earthquake damage and losses, in terms of building downtime, costly repairs and even injuries to the occupants. Nevertheless, research and literature on the seismic performance of cable-net façades are still very limited.*

In this study, the seismic response of a cable-net glass façade under earthquake excitation is investigated. A case study concerning a façade originally designed without considering the seismic loading is presented. A finite element model of the façade is developed, fully accounting for the geometric nonlinearity in the mechanical behaviour of pre-tensioned cables under large displacements. Nonlinear response history analyses under earthquake excitation are carried out by direct numerical integration of the equations of motion. Seismic input is modelled by way of artificial accelerograms matching the pseudo-acceleration elastic design spectra given by Eurocode 8. Increasing levels of the design peak ground acceleration and five different ground types are considered to derive the elastic design spectra and to generate the artificial accelerograms. Numerical simulations aim at exploring the influence of the intensity and frequency content of seismic input on the façade response. According to Eurocode 8 provisions, response parameters of the façade are evaluated in terms of statistical averages across a set of seven records per each analysis. Out-of-plane displacements and absolute accelerations of the façade, variations of the tension force in the cables, and incremental loads in the connection joints are examined.

1 Introduction

An increasing number of modern iconic architectures are adopting cable-net glass façades, which employs a net of orthogonal pre-tensioned steel cables to support glazing units: well-known examples, among the others, are the Market Hall in Rotterdam and the Sony Centre building in Berlin (Figure 1). While, on the one hand, the lightness of the supporting system has an architectural and aesthetic value, on the other hand it can cause large deflections of the façade under horizontal loadings and vulnerability to earthquake damage. According to the taxonomy of nonstructural building components given by FEMA E-74 (FEMA 2012), glass façades are classified as architectural components and the consequences of their earthquake damage are considered significant with respect to three types of risk: serious falling hazard with subsequent injuries and casualties (life safety risk); repair and replacements costs (property loss); obstruction

(a) (b)

Figure 1. Examples of cable-net glass façades: (a) Market Hall, Rotterdam (© W. Bulach / Wikimedia Commons / CC-BY-SA-4.0); (b) Sony Centre, Berlin (© Andreas Steinhoff / Wikimedia Commons).

of egress routes (functional loss). Nevertheless, research and literature on the seismic performance of cable-net glass façades are still very limited.

This paper aims at investigating the seismic performance of a cable-net glass façade originally designed without considering the seismic loading. In Section 2, a general description of the façade is given and its finite element modelling is dealt with. In Section 3, seismic analyses carried out on the façade model are presented and discussed. Nonlinear response history analyses with direct numerical integration of the equations of motion are performed, fully accounting for the geometric nonlinearity in the mechanical behaviour of pre-tensioned cables under large displacements. Earthquake excitation is modelled by way of artificial accelerograms generated to match the pseudo-acceleration elastic design spectra given by the European standard Eurocode 8 EN 1998-1:2004 (CEN 2004). Increasing levels of the design peak ground acceleration and five different ground types are considered to derive the elastic design spectra. In Section 4, conclusions from the present study and suggestions for future research are drawn.

2 Cable-net glass façade

2.1 General description

A cable-net glass façade 29 m high and 14.3 m wide is considered in the present study (Figure 2a).

The wall glazing is made of double insulated glass units (IGUs) having a width of 1200 mm and a height in the range 1925-2075 mm. Each double IGU is composed by an external 2-ply heat strengthened laminated glass pane, a cavity filled with argon and an internal 2-ply heat strengthened laminated glass pane. Thicknesses are 17.52 mm for the external glass pane, 16 mm for the cavity and 9.52 mm for the internal glass pane.

The wall glazing is supported by a net of orthogonal prestressed stainless-steel cables. Each IGU is connected to the cable-net by way of machined stainless-steel clamping patch fittings at the four corners. Horizontal and vertical gaps between adjacent glass panels are sealed by a vented double silicone sealing. The cable-net system is then anchored to two vertical S355 steel truss beams on the façade edges, a horizontal S355 steel truss beam on the top and a continuous concrete beam on the bottom. The vertical steel trusses are fixed at the base and constrained along the elevation to four building slabs. The horizontal steel truss is connected to the vertical steel trusses via pinned constraints. Pre-tension is applied to increase the stiffness of the cables and to limit the deflections of the façade.

Regarding the load path, the dead load of the IGUs is totally transmitted to the vertical steel cables. Vertical cables are 29 m long, composed of a stainless-steel strand of 10 mm diameter and pre-tensioned with a load of 30 kN. The wind load acting on the glass units is transmitted to the horizontal steel cables. Horizontal cables are 15 m long, composed of a stainless-steel strand of 32 mm diameter and pre-tensioned with a load of about 346 kN. Horizontal cables are wind resisting elements.

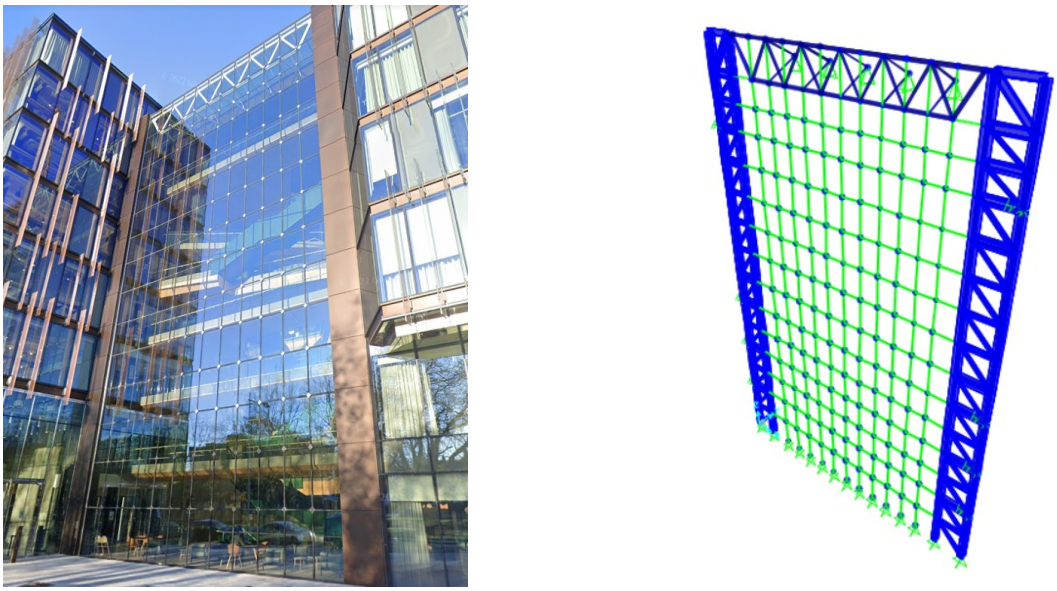

(a) (b)

Figure 2. The cable-net glass façade: (a) front view; (b) FE model of the façade system developed using the structural analysis program SAP2000 v.24 (Computers & Structures 2022).

2.2 Modelling

A Finite Element (FE) model (Figure 2b) of the cable-net façade has been developed by employing the structural analysis program SAP2000 v.24 (Computers & Structures 2022). A global coordinate system is introduced with the x-axis as horizontal and parallel to the façade plane, the y-axis as horizontal and orthogonal to the façade plane, the z-axis as vertical and positive upwards.

The cable-net is modelled using the *cable element* to simulate the cables. The cable element is characterised by a highly nonlinear behaviour that inherently includes tension-stiffening and large-deflection effects. Prestress on cables is applied as a *target-force load,* a type of loading which iteratively applies deformation loads to the cable in order to achieve a target internal tension force. The members of the vertical and horizontal steel truss beams, which cables are anchored to, are modelled using the *beam element*. Restraint conditions on the façade system are applied to the vertical truss beams and at the bottom end of vertical cables.

Previous literature studies have demonstrated that the contribution of glass panels and sealing to the global stiffness of a cable-net façade is negligible (Xiang *et al.* 2020, Wang *et al*. 2019, Feng *et al*. 2013, Feng *et al*. 2009, Feng *et al*. 2007). Based on this consideration, glass panels are modelled as concentrated masses at each node of the cable-net, i.e. at each intersection point between vertical and horizontal cables. Lumped nodal masses amount to different values in the range 108-154 kg depending on the dimensions of the glass panels connected to a given node.

Damping of the façade system is modelled according to the Rayleigh proportional damping model, by specifying a modal damping ratio of 0.02 corresponding to frequencies 1.78 Hz and 2.10 Hz.

Table 1 lists the properties associated to the first ten natural vibration modes of the cable-net glass façade: modal periods and frequencies; modal and cumulative participating mass ratios in the out-of-plane direction (y-axis). Vibration modes that contribute the most in terms of participating mass ratios are the 1st, the 3rd and the 5th, which are characterised by modal shapes symmetrical with respect to the central horizontal line of the façade (Figure 3). The cumulative participating mass ratio corresponding to the first ten vibration modes is 37%, a value that may appear not sufficiently high to provide accurate results in simulating the seismic response of the façade. The value 37% is explained by the fact that the modes in Table 1 excite only the masses of cable-net and glass panels and not the masses (way larger) of the supporting truss beams. In this regard, modes of Table 1 have been compared with the modes of a second FE model that includes only cable-net and glass panels and not the supporting truss beams. The modes of this second FE model overlap the modes of Table 1 except for the participating mass ratios, which are much higher, with a cumulative participating mass ratio equal to 95% corresponding to first ten modes.

Table 1. Modal periods and frequencies, modal and cumulative participating mass ratios in the out-of-plane direction for the first ten natural vibration modes of the cable-net glass façade.

Modes	Periods (s)	Frequencies (Hz)	Participating mass ratios (%)	Cumulative participating mass ratios (%)
1	0.561	1.784	30.00	30
2	0.521	1.921	0.62	31
3	0.477	2.097	4.06	35
4	0.431	2.320	0.10	35
5	0.390	2.563	1.10	36
6	0.356	2.807	0.04	36
7	0.329	3.042	0.57	37
8	0.307	3.263	0.02	37
9	0.288	3.475	0.19	37
10	0.286	3.495	0.00	37

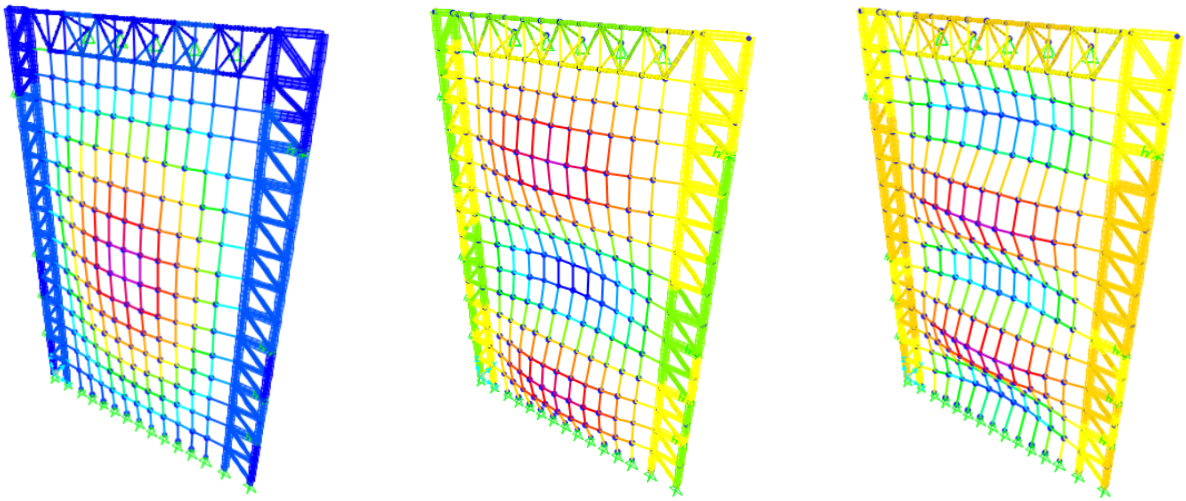

(a) (b) (c)

Figure 3. Mode shapes of the cable-net glass façade: (a) 1st mode; (b) 3rd mode; (c) 5th mode.

3 Seismic analyses

The seismic response of the cable-net glass façade has been studied by carrying out on the FE model in SAP2000 nonlinear time history analyses with direct integration of the equations of motion. Geometric nonlinearity is accounted for by considering P-Delta and large displacements effects and using Newton-Raphson iterations.

3.1 Earthquake excitation

Earthquake excitation is modelled by way of ground acceleration time histories applied to the restraint supports of the cable-net glass façade along the out-of-plane direction (y-axis). Artificial accelerograms are used, generated by software SIMQKE (NISEE 1990) to match elastic design spectra given by Eurocode 8.

Pseudo-acceleration elastic design spectra for the horizontal components of seismic action and 5% damping ratio are considered. The spectrum shape is given by mathematical function $S_e(T)$, being S_e the spectral ordinate and T the natural vibration period of a single-degree-of-freedom system. Function $S_e(T)$ is characterised by four parameters that depend upon the ground type. Such parameters are: T_b, T_c and T_d, which denote, respectively, the periods at the beginning of the constant-pseudo-acceleration, constant-pseudo-velocity and constant-deformation regions of the spectrum; S, a multiplier to obtain the design Peak Ground Acceleration (PGA) Sa_g for the given ground type, where a_g is the design PGA for rock ground. Five ground types are accounted for: A (rock), B (very stiff soil), C (medium stiff soil), D (soft soil), E (thin stratum of medium/soft soil over rock). Figure 4a illustrates the normalised pseudo-acceleration elastic design spectra $S_e(T)/a_g$ for the five ground types.

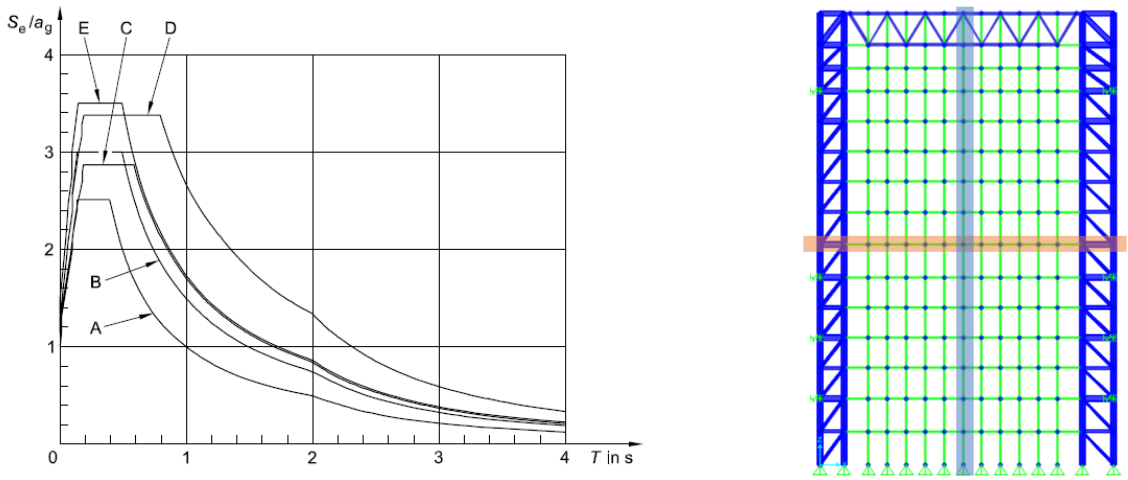

(a) (b)

Figure 4. Seismic analyses: (a) normalised pseudo-acceleration elastic design spectra $S_e(T)/a_g$ for 5% damping ratio and five ground types (A-rock, B-very stiff soil, C-medium stiff soil, D-soft soil, E-thin stratum of medium/soft soil over rock) according to Eurocode 8 (CEN 2004), being a_g the design PGA on type A ground; (b) highlighted in colour, the horizontal and vertical cables monitored in the seismic analyses.

In this study, 15 pseudo-acceleration elastic design spectra have been considered in total, encompassing: three levels of seismic excitation, corresponding to three values of the design PGA on type A ground, a_g, respectively $0.15g$, $0.25g$ and $0.35g$, being g the gravity acceleration; and five ground types (A, B, C, D, E). The design PGA Sa_g for each of the considered 15 spectra, i.e., for each combination of the 3 seismic excitation levels and the 5 ground types, is shown in Table 2.

Table 2. Design PGA Sa_g for the 15 pseudo-acceleration elastic design spectra (5% damping) considered in this study.

	Design PGA on type A ground a_g (g)	**Ground type**				
		A	**B**	**C**	**D**	**E**
Design PGA Sa_g (g)	0.15	0.15	0.18	0.17	0.20	0.23
	0.25	0.25	0.30	0.29	0.34	0.38
	0.35	0.35	0.42	0.40	0.47	0.53

For each of the considered 15 spectra, a suite of 7 statistically independent artificial accelerograms have been generated. A total duration of 20 s with a stationary part lasting 10 s have been set for the generated accelerograms. According to Eurocode 8 provisions, the match with the elastic design spectrum is guaranteed by the following requirement: in the range of periods between $0.2T_1$ and $2T_1$, where $T_1 = 0.561$ s is the fundamental period of the cable-net façade, no value of the mean 5% damping elastic response spectrum, calculated from all the accelerograms of the suite, is less than 90% of the corresponding value of the 5% damping elastic design spectrum.

3.2 Results and discussion

The FE model of the cable-net glass façade has been subjected to 15 sets of seismic analyses. Each set includes 7 nonlinear time histories analyses with the artificial accelerograms generated from one of the 15 elastic design spectra described in the previous paragraph. To assess the seismic response of the façade, two representative cables are selected, one vertical at mid-width and one horizontal at mid-height of the façade, highlighted in Figure 4b. Monitored response parameters are: displacements and absolute accelerations of the cable nodes in the out-of-plane direction (y-axis); cable internal axial force (tension); loads in the clamping patch fittings between cables and glass units. As an example, Figure 5 illustrates one artificial accelerogram used as seismic input to the façade as well as the corresponding time history responses in terms of: displacements and absolute accelerations of the central node of the monitored horizontal cable; tension force in the monitored horizontal cable. Time histories are therefore elaborated to determine the maximum absolute (peak) and Root Mean Square (RMS) values of the responses. According to Eurocode 8, such response values from one set of 7 nonlinear time histories analyses are computed as the average of the values obtained from the 7 analyses.

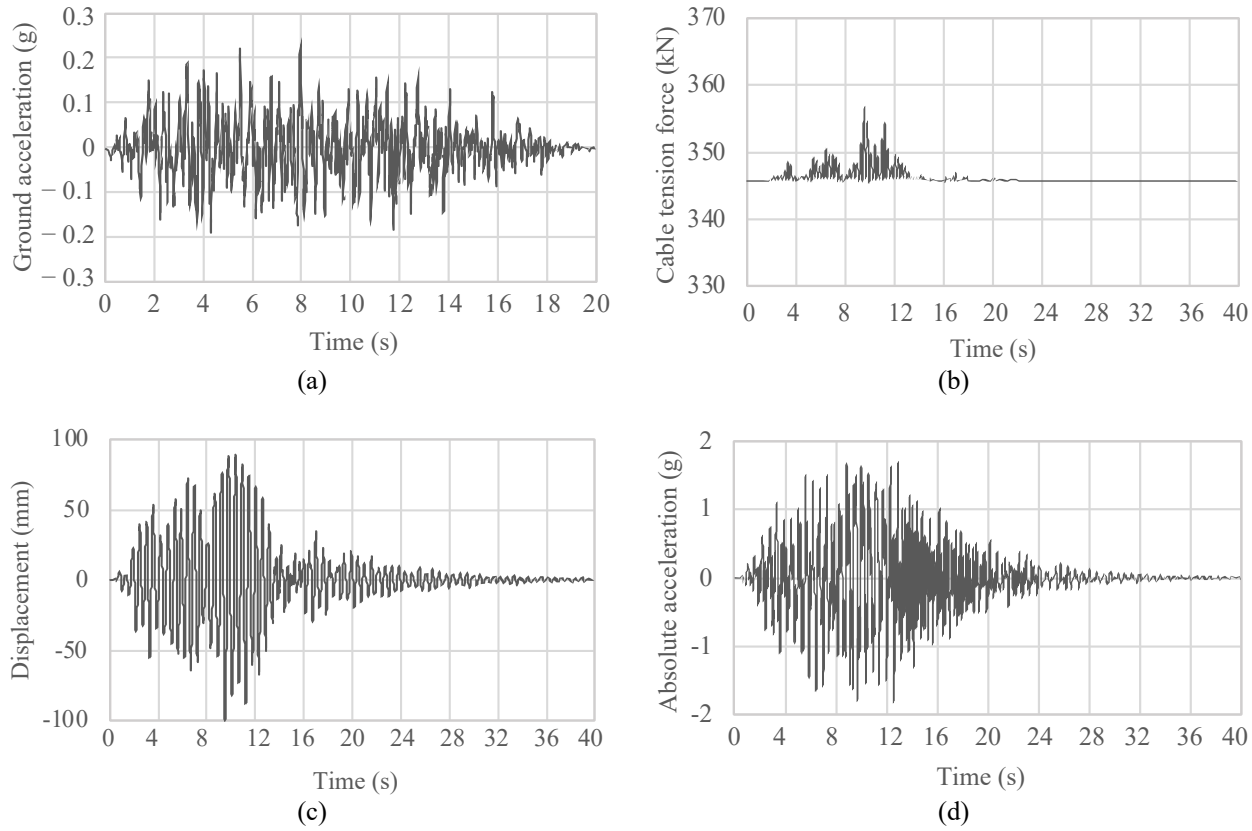

Figure 5. A single nonlinear time history analysis with type A ground and design PGA for type A ground $a_g = 0.25g$: (a) generated artificial accelerogram used as seismic input to the façade; (b) tension force in the monitored horizontal cable (c) displacement response of the central node (node 7) of the monitored horizontal cable; (d) absolute acceleration response of the central node (node 7) of the monitored horizontal cable.

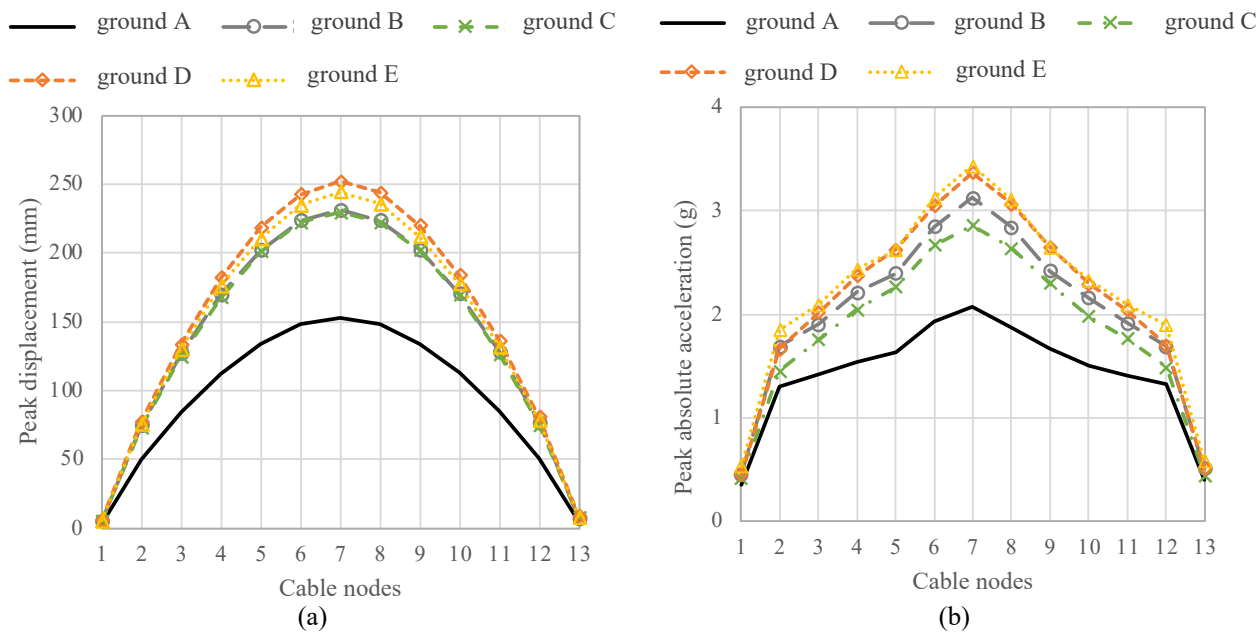

Figure 6. Seismic analyses setting the design PGA for type A ground $a_g = 0.35g$ and varying the ground type, profiles of peak nodal responses along the monitored horizontal cable: (a) displacements; (b) absolute accelerations.

In the following, results from the nonlinear time history analyses are reported and discussed.

Figure 6 illustrates the profiles, along the monitored horizontal cable, of the peak values of nodal displacements and absolute accelerations. Results from seismic analyses carried out by setting the same excitation level (design PGA on type A ground $a_g = 0.35\ g$) and varying the ground type are reported. Profiles are substantially symmetrical and increasing from the sides to the central node of the cable, denominated as node 7. A slight dissymmetry appears in the acceleration profile, due to the different geometry of the vertical truss beams at the edges of the façade. Variations with the ground type are highlighted, with higher peak values corresponding to ground types D and E, both for nodal displacements and nodal absolute accelerations. As apparent from Figure 4a, the pseudo-acceleration elastic design spectra for type D and E grounds present the greatest spectral amplifications and, in case of type D ground, also the largest constant-pseudo-acceleration region of the spectrum.

Tables 3 and 4 show the peak values, respectively, of displacement and absolute acceleration for the central node (node 7) of the monitored horizontal cable, with varying both the seismic excitation level and the ground type. Significant variations of the responses with varying ground types are confirmed for all the investigated excitation levels. As to the peak nodal displacements, the increase from type A to type D ground is 76% when $a_g = 0.15\ g$ (65.7 mm *vs* 115.9 mm), 72% when $a_g = 0.25\ g$ (109.4 mm *vs* 188.4 mm) and 65% when $a_g = 0.35\ g$ (153 mm *vs* 251.9 mm). To establish a comparison, the limit value usually assumed in the design of cable-net glass façades for cable displacements under wind load is equal to 1/50 of the cable length: in the case of the monitored horizontal cable, cable length is 15 m and such a limit value is equal to 300 mm. As to the peak nodal absolute accelerations, the increase from type A to type E ground is 67% when $a_g = 0.15\ g$ (1.2 g *vs* 2.0 g), 63% when $a_g = 0.25\ g$ (1.6 g *vs* 2.6 g), 62% when $a_g = 0.35\ g$ (2.1 g *vs* 3.4 g).

Table 3. Peak displacements of the central node (node 7) of the monitored horizontal cable.

	Design PGA on type A ground a_g (g)	**Ground type**				
		A	**B**	**C**	**D**	**E**
Peak nodal displacement (mm)	0.15	65.7	99.4	100.1	115.9	112.1
	0.25	109.4	165.2	164.1	188.4	182.6
	0.35	153.0	231.0	229.6	251.9	244.2

Table 4. Peak absolute accelerations of the central node (node 7) of the monitored horizontal cable.

	Design PGA on type A ground a_g (g)	**Ground type**				
		A	**B**	**C**	**D**	**E**
Peak nodal absolute acceleration (g)	0.15	1.2	1.7	1.7	1.9	2.0
	0.25	1.6	2.1	2.3	2.6	2.6
	0.35	2.1	3.1	2.9	3.4	3.4

Table 5 indicates the peak values of the tension force in the monitored horizontal cable with varying seismic excitation levels and ground types. It is shown that the total internal force in the cable, which includes both the pre-tension of about 346 kN and the earthquake-induced tension, does not change significantly with respect to pre-tension, with a maximum increase of 17%. Table 6 shows the peak values of the load in the clamping joint corresponding to the central node (node 7) of the monitored horizontal cable, with varying seismic excitation levels and ground types. Considering that the maximum horizontal force used to design the considered cable-net glass façade, due to the wind pressure, is about 2.9 kN per each node, the resistance of the clamping joints under the effect of the seismic excitation should be verified.

Table 5. Peak tension force in the monitored horizontal cable.

	Design PGA on type A ground a_g (g)	**Ground type**				
		A	**B**	**C**	**D**	**E**
Peak cable tension force (kN)	0.15	350.4	356.4	356.3	359.9	359.2
	0.25	358.8	374.8	373.6	381.8	380.4
	0.35	371.3	387.8	386.5	406.4	404.9

Table 6. Peak load in the clamping joint corresponding to the central node (node 7) of the monitored horizontal cable

	Design PGA on type A ground a_g (g)	**Ground type**				
		A	**B**	**C**	**D**	**E**
Peak clamping load (kN)	0.15	1.753	2.518	2.407	2.780	2.846
	0.25	2.336	2.959	3.331	3.807	3.807
	0.35	2.978	4.505	4.119	4.851	4.945

4 Conclusions

In this paper, a cable-net glass façade originally designed without considering the seismic loading has been dealt with and its seismic performance has been investigated by way of numerical simulations on a FE model. Nonlinear direct-integration response history analyses have been carried out by using artificial accelerograms generated to match elastic design spectra given by Eurocode 8. Seismic analyses have highlighted the influence of the intensity and frequency content of earthquake excitation of the façade response.

Future research developments will include the analysis of cable-net glass façades under earthquake excitation applied both along the in-plane and the out-of-plane direction. The filtering effect exerted by a building frame structure, which the façade is anchored to, on the seismic input received by the façade will also be investigated, posing a problem of multiple-support earthquake excitation (Chopra 2022).

5 References

Chopra A. (2022). *Dynamics of Structures. Theory and Applications to Earthquake Engineering*, 6th Ed., Pearson Education, Upper Saddle River, NJ, USA.

Computers & Structures Inc. (2022). *SAP2000 Release 24 Documentation*, Berkeley, CA, USA.

European Committee for Standardisation (CEN) (2004). *Eurocode 8: Design of structures for earthquake resistance – Part 1: General rules, seismic actions and rules for buildings*, EN 1998-1:2004, Brussels, Belgium.

Federal Emergency Management Agency (FEMA) (2012). *Reducing the Risks of Nonstructural Earthquake Damage - A Practical Guide*, FEMA E- 74:2012, Washington, D.C., USA.

Feng R-Q., Wu Y., Shen S-Z. (2007). Working mechanism of single-layer cable net supported glass curtain walls. *Advances in Structural Engineering*, 10(2):183–95.

Feng R-Q., Zhang L-l., Wu Y., Shen S-H. (2009). Dynamic performance of cable-net facades. *Journal of Constructional Steel Research*, 65: 2217–2227.

Feng R-Q., Ye J., Yan G., Ge J-M. (2013). Dynamic nonlinearity and nonlinear single-degree-of- freedom model for cable net glazing. ASCE Journal of Engineering Mechanics, 139(10):1446–59.

NISEE software library (1990). *SIMQKE-I: Simulation of Earthquake Ground Motions*, User Manual by Vanmarcke, E. H., Cornell, C. A., Gasparini, D. A., Hou, S-n., Pacific Earthquake Engineering Research (PEER) Center, University of California, Berkeley, CA, USA.

Xiang Y., Zhang Y-J., Guo J., Chen J. (2020). Effect of the primary structure on the seismic response of the cable-net façade. *Engineering Structures*, 220:110989.

Wang Y., Wang Z., Xu K., Shi Y., Du X. (2019). Experimental and numerical studies on the static and the dynamic behaviors of embedded cable support (ECS) glass façade system. *Engineering Structures*, 178:521-533.